Collaborative Computing of Urban Built-Up Area Identification from Remote Sensing Image

Chengfan Li[1,2(✉)], Lan Liu[3], Yongmei Lei[1], Xiankun Sun[3], and Junjuan Zhao[1]

[1] School of Computer Engineering and Science, Shanghai University, Shanghai 200444, China
david-0904@163.com
[2] Shanghai Institute of Advanced Communication and Data Science, Shanghai University, Shanghai 200444, China
[3] School of Electronic and Electrical Engineering, Shanghai University of Engineering Science, Shanghai 201620, China

Abstract. Urban built-up area is one of the important criterions of urbanization. Remote sensing can quickly acquire dynamic temporal and spatial variation of urban built-up area, but how to identify and extract urban built-up area information from massive remote sensing data has become a bottleneck arousing widespread concerns in the field of the data mining and application for remote sensing. Based on the traditional urban built-up area identification and data mining of remote sensing, this paper proposed a new collaborative computing method for urban built-up area identification from remote sensing image. In the method, the normalized difference built-up index (NDBI) and the normalized differential vegetation index (NDVI) feature images were constructed firstly from the spectrum clustering map; and then the urban built-up area was identified and extracted by the map-spectrum synergy and mathematical morphology methods. Finally, a case of collaborative computing of urban built-up areas in Chongqing city, China is presented. And the experimental results show that the total accuracy of urban built-up area identification in 1988 and 2007 reached 92.58% and 91.41%, the Kappa coefficient reached 0.8933 and 0.8722, respectively, and the good results in the temporal and spatial variation monitoring of urban built-up area are achieved.

Keywords: Remote sensing image · Collaborative computing · Urban built-up area · Map-spectrum synergy

1 Introduction

In recent years, with the sustained and rapid growth of China's economy, the urbanization continues to increase. Statistically, the total area of urban built-up area in China was about 2×10^5 km^2 by 2017, and the urbanization rate reached 58.52% [1]. How to accurately obtain the dynamic range of urban built-up area has become an urgent task of urban construction and management [2–4]. There are many methods to identify and

X. Wang et al. (Eds.): CollaborateCom 2019, LNICST 292, pp. 260–278, 2019.
https://doi.org/10.1007/978-3-030-30146-0_18

extract the urban built-up area at present, among the methods, the nighttime lighting monitoring from remote sensing image is the most influential and representative [5–7]. However, the traditionally methods which rely on a single means to identify urban built-up area is unrealistic and impractical because of the influence by saturation diffusion and threshold selection. In addition, the urban built-up area is a complex affected by human political, economic and social activities. There are many types of land objects, e.g., buildings, roads, grasslands, rivers, mountains, construction sites, forest land, etc., and the random confusion of different types of objects is obvious. Meanwhile, how to identify and extract the urban built-up area has become a focus of the authorities and the related department.

With the development of space-to-earth observation and the continuous improvement of sensor performance, remote sensing can quickly capture the change information of earth surface with advantages of multi-source, multi-angle and multi-resolution, and has the characteristics of fast data acquisition, short update period and strong timeliness. Accordingly, the amount of remote sensing data has shown an exponential growth trend and has entered the era of big data [8–10]. However, it has a relatively weak ability of data processing in the remote sensing big data and causes data redundancy and dimensional disaster, how to accurately analyze the massive remote sensing data and find out the urban built-up area has become the main focus of urban built-up area dynamic monitoring from remote sensing images. The collaborative computing was first used in the fields of computer networks, resource scheduling, communication, and multimedia, etc. At present it has been widely used in many fields and industries [11]. It has been introduced into the remote sensing only in decades. Limited by the accuracy and efficiency of remote sensing data mining, Chen et al. [12] firstly proposed the idea of geoscience information map-spectrum, and laid the foundation for the full implementation of collaborative computing of remote sensing data mining with the formation of remote sensing big data. Luo et al. [13] explored the cognitive theory of remote sensing map-spectrum and calculation, and pointed out that it is feasible to develop remote sensing cognitive theory and methods combined with visual cognition. Shen et al. [14] extract the Baiyangdian wetland information from the remote time data by the collaborative computing method, and pointed out that the area of Baiyangdian wetland began to reduce firstly and later increase the science 1973. Li et al. [1] extracted the urban built-up area of Beijing-Tianjin-Hebei region from remote sensing images by the comprehensive utilization of multi-source remote sensing data and DMSP/OLS data, and the effectiveness of collaborative computing in the extraction of urban built-up area is verified by the overall accuracy and Kappa coefficient. In general, although collaborative computing can provide a new perspective for remote sensing data mining and information identification of interest, collaborative analysis from multiple data, methods and knowledge enables the extraction and analysis of hidden information [15, 16], so far, the collaborative computing in remote sensing image data mining is still in its infancy, and the related achievements are few.

As the youngest municipality in China, Chongqing has experienced rapid economic development in recent years. At the same time, the urban built-up area covers an area of 150 km^2 in 1988 and 700 km^2 in 2018, respectively. On the basis of the systematic summarization of the map and spectrum information in remote sensing, taking Chongqing main urban area as an example, this paper presented a new collaborative

computing method integrating into different levels of knowledge to identify urban built-up area from remote sensing images. The specific collaborative computing includes algorithms, computing resources and computing modes in the process of the calculation, remote sensing data, information, features and knowledge. It can identify accurately the dynamic change information of urban built-up area and improve effectively the remote sensing data mining.

Work in this study is focused on the collaborative computing of map-spectrum synergy for urban built-up area from remote sensing images. The rest of the paper is constructed as follows: Sect. 2 describes brief collaborative computing method of urban built-up area identification and extraction. Section 3 presents a case of collaborative calculation of urban built-up area from remote sensing image. Section 4 devotes the results and analysis. Finally, the discussions and conclusions are separately drawn in Sects. 5 and 6.

2 Collaborative Computing Method of Urban Built-Up Area Identification and Extraction

2.1 Collaborative Computing Mode of Remote Sensing Information

(1) Map-Spectrum Collaborative Computing
Remote sensing images contain plentiful map and spectrum information [17, 18]. The map, also known as spatial information, refers to the shape of the research unit and the spatial relationship and configuration among different units, i.e., pixels, parcels. The spectrum contains spectral, band information, time spectrum, feature attribute spectrum, knowledge spectrum and other forms of the same unit in different dimensions, i.e., spectral performance and long-term phase change information. Map-spectrum collaborative computing is an important basis for the classification and thematic information extraction from remote sensing image.

(2) Multi-resolution and Multi-temporal Collaborative Computing
It is the manifestation of map-spectrum collaborative computing. Multi-resolution synergy realizes collaborative computing of multi-source and multi-resolution data by comprehensively utilizing high-resolution, medium-resolution and low-resolution remote sensing images. Multi-temporal synergy detects changes by collaborative computing multiple time-point remote sensing images [19–22]. Synthesizing remote sensing image information of different resolutions and multi-temporal can provide more accurate and rich map-spectrum information, and it is easy to improve the accuracy of classification and thematic information extraction and change detection from remote sensing images.

(3) Multi-knowledge and Multi-algorithm Collaborative Computing
In the course of remote sensing image processing, on the basis of assisting different levels of prior knowledge, it is necessary to improve the accuracy of remote sensing image classification and thematic information extraction by collaborative computing of multiple knowledge [23, 24]. Such as the spatial relationship between the earths surfaces objects, the reasoning mechanism, the configuration method, the causal relationship and

other knowledge models, etc. In addition, the collaborative computing of multiple algorithms improves the efficiency and reliability of remote sensing image mining to a certain extent. There are many usual varieties of indices in the collaborative computing and classification of remote sensing image, i.e., normalized differential vegetation index (NDVI), ration vegetation index (RVI), difference vegetation index (DVI), etc.

2.2 Collaborative Computing of Urban Built-Up Area Identification

The specific collaborative computation method of urban built-up areas from remote sensing images in this paper mainly includes the following steps:

(1) Data Preprocessing
In this study, data preprocessing mainly contains geometric correction and cloud removal. In the data processing, the parameters from geographic position data set were first extracted and used to perform the geometric correction, and then the calibration data set was obtained. Next, the respectively bands R(red), B(blue) and G(green) were selected from remote sensing dataset and further generated a sample dataset, and then a corrected total dataset was obtained by stacking. For the ETM and TM remote sensing data with thin cloud, the cloud removal was performed by cloud mask data.

(2) From Spectrum Clustering Map, Constructing Feature Images of Normalized Difference Built-Up Index (NDBI) and NDVI
Due to the NDBI has a good recognition characteristics of the global built-up area, and it is easy to identify the urban built-up area as a whole. The NDBI computation is as shown below:

$$NDBI = \frac{MIR - NIR}{MIR + NIR} \tag{1}$$

where MIR and NIR are pixel luminance values in the mid-infrared and near-infrared bands, respectively. For the TM sensor, it corresponds to Band 5 and Band 4, respectively.

Similarly, the NDVI is an effective indicator for the coverage of ground vegetation and is widely used in the field of vegetation information extraction. The specific NDVI computation is as shown below:

$$NDVI = \frac{NIR - \mathrm{Re}\, d}{NIR + \mathrm{Re}\, d} \tag{2}$$

where NIR and Red are the pixel luminance values of the near-infrared band and the red-light band, which correspond to the band 4 and band 3 of the TM sensor, respectively.

(3) Map-Spectrum Collaborative Computing, Preliminary Identification of Urban Built-Up Area
Based on the administrative boundary of the study area, the total area of the built-up area within the administrative boundary is statistically calculated. Then the regional segmentation method is used to calculate the optimal segmentation threshold of the

different administrative units in NDBI feature images, and the spatial distribution information of the urban built-up zone boundaries is obtained. The specific calculation formula is as shown below:

$$\Delta S_k(T_i) = S_k - S_k(T_0 - i) \tag{3}$$

where T_0 is initial threshold value, i is the step size, and $i = 0.1, 0.2, 0.3 \cdots$; k is the k-th administrative boundary in the research area, and $k = 1, 2, 3, \cdots$; S_k is the statistical value of area of administrative boundary, $S_k(T_0 - i)$ is the identified area from feature images, $\Delta S_k(T_i)$ is the difference between identification area and statistical area of the same administrative boundary. If $\Delta S_k(T_i)$ satisfy the condition $\Delta S_k(T_i) < \Delta S_k(T_{i+0.1}) \cap \Delta S_k(T_i) < \Delta S_k(T_{i-0.1})$, then T_i is the optimal segmentation threshold of k-th administrative boundary.

(4) Map-Spectrum Collaborative Computing, Further Identification of Urban Built-Up Area

Based on the preliminary identification of urban built-up areas, multi-scale segmentation algorithm is used to further identify the urban built-up areas from remote sensing image. And the specific calculation formula is as shown below:

$$dH = dH_{color} w_{color} + dH_{shape} w_{shape} \tag{4}$$

where dH is the heterogeneity index of multi-scale segmentation; dH_{color} and w_{color} is the spectral heterogeneity index and weight value, respectively; dH_{shape} and w_{shape} is the shape heterogeneity index and weight value, respectively.

Subsequently, the regional loop identification method is used to number the results of the newly identified urban built-up areas, and the maximum and minimum values of NDVI in each unit are calculated and regarded as the upper and lower thresholds of the urban built-up area. The specific formula is as shown below:

$$\begin{cases} NDVI_{A_i threshold\_\max}(x) = \max\{NDVI_{S_i}(x)\} \\ NDVI_{A_i threshold\_\min}(y) = \min\{NDVI_{S_i}(y)\} \end{cases} \tag{5}$$

where A_i is the i-th administrative unit, S_i is the identified i-th urban built-up area, $NDVI_{A_i threshold\_\max}(x)$ and $NDVI_{A_i threshold\_\min}(y)$ are the upper and lower value of segmentation threshold, respectively. And then the attribute of earth object is acquired by the judging criteria. That is to say, when $S_i(t)$ is judged as the type of the urban built-up area $NDVI_{S_i(t)} \in (NDVI_{A_i threshold\_\min}(y), NDVI_{A_i threshold\_\max}(x))$.

(5) Mathematical Morphology Post Processing

The mathematical morphology operators used in this study are mainly composed of open operations and expansion operations. And the specific calculation formula is as shown below:

$$\begin{cases} A \circ B = (A \Theta B) \oplus B \\ A \oplus B = \left\{ x | ((\hat{B})_y \cap A) \neq \emptyset \right\} \end{cases} \tag{6}$$

where A and B are two non-empty sets, $\hat{B}$ is the mapping of sets B, $\hat{B} = \{x|x = -b, b \in B\}$, y is the displacement of $\hat{B}$, namely, $\hat{B}_y = \{y|y = b + x, b \in B\}$.

The expansion operation was used to the later identified urban built-up area, and the gaps and breaks in the middle of the image and some broken maps of the walk were deleted. Meanwhile, the expansion image was refined further by the open operation. And then the distribution and statistical information of the urban built-up area are finally obtained.

3 Collaborative Calculation Case of Urban Built-Up Area

3.1 General Situation of Research Area

Chongqing is located in the eastern part of the Sichuan Basin, China. It is situated in the junction zone between the eastern part of China and the western part. The main urban area in Chongqing is shown in Fig. 1. The urban area of Chongqing usually includes the area among the Yangtze River, Jialing River, Zhongliang Mountain and Tonglu Mountain. The total area is about 700 km^2. The terrain in the area is dominated by low mountains and hills, and has an average elevation of about 400 m. Since the establishment of the municipality in 1997, the economy in Chongqing has developed rapidly and the scale of the urban built-up area has expanded rapidly. And now it has formed a new spatial distribution pattern with multi-center and group.

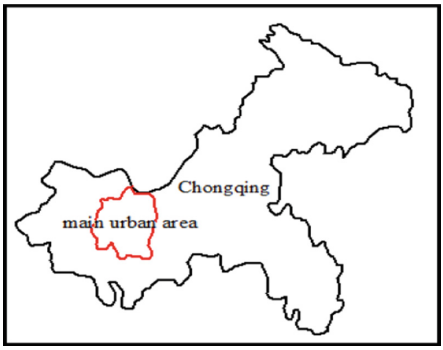

Fig. 1. Geographical location of the main urban area.

3.2 Data Collection

(1) Remote Sensing Data

The remote sensing data contains the medium resolution thematic mapper (TM) images in 1988 and 2007, respectively, and the imaging season is roughly the same. Due to the sixth band in TM sensor is a thermal infrared band and has low spatial resolution of 120 m. it usual affected severely by the atmosphere, so in this study it is not involved in band synthesis. The main parameters of TM sensor are shown in Table 1.

Table 1. Performance of sensors

Time	Band	Resolution (m)	Wavelength (μm)	min	max	avg	med	Standard deviation
1988	1	30	0.45–0.52	77	254	107.21	104	11.48
	2	30	0.52–0.60	26	145	44.60	43	5.60
	3	30	0.63–0.69	21	179	46.07	44	9.66
	4	30	0.76–0.90	15	208	66.45	66	14.67
	5	30	1.55–1.75	2	254	59.72	61	19.45
	7	30	2.08–2.35	1	254	24.05	25	8.14
2007	1	30	0.45–0.52	73	196	96.24	96	8.05
	2	30	0.52–0.60	28	105	42.08	41	4.69
	3	30	0.63–0.69	24	134	42.20	40	8.05
	4	30	0.76–0.90	24	128	64.42	65	13.44
	5	30	1.55–1.75	13	255	63.58	66	16.57
	7	30	2.08–2.35	3	255	29.231	28	11.00

(2) Thematic Data

The thematic data includes the digital topographic maps in Chongqing with 1:50000 scales and the digital elevation model (DEM) in Chongqing. Social data includes the natural and socioeconomic survey statistics. The collected thematic data is usual used to the geometric correction, verification and correction after the classification of remote sensing image. In addition, in this study we also involved in the landuse map of Chongqing in 1983, 1994, 2000 and 2003, respectively (see Fig. 2).

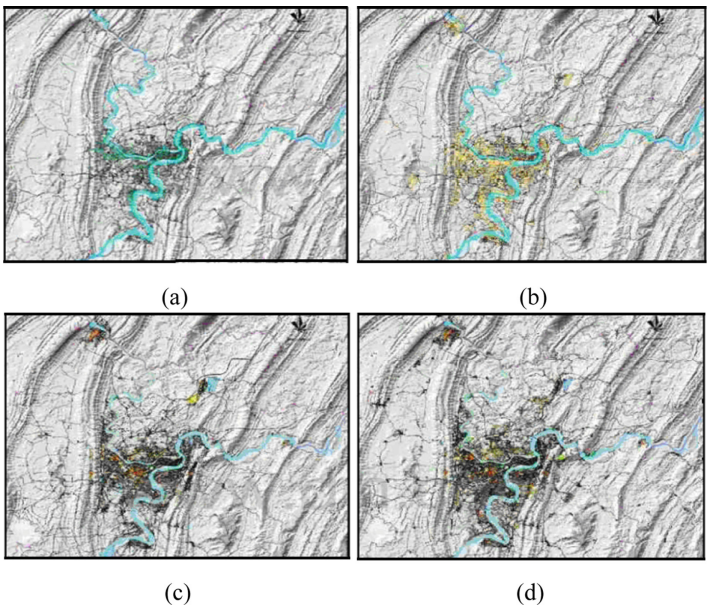

Fig. 2. Landuse maps, (a) 1983, (b) 1994, (c) 2000, (d) 2003.

(3) Data Preprocessing

Remote sensing image preprocessing process mainly includes filtering noise, radiation correction, geometric correction, image registration, fusion and enhancement. Therinto, the key is geometric correction and image registration.

In addition, for remote sensing images with different imaging time, in order to make the pixels brightness of remote sensing image in different phases consistent and have the comparable and same geospatial coordinate reference and spatial resolution, it is also necessary to perform radiation correction, normalization and resampling processing so as to make. The preprocessed TM remote sensing images are shown in Fig. 3.

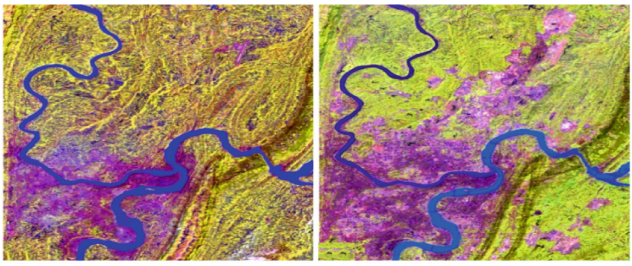

(a) (b)

Fig. 3. Preprocessed TM images, (a) 1988, (b) 2007.

As can be seen from Fig. 3, there is a brilliant color and a strong sense of layering in the preprocessed TM remote sensing images. The image contrast and inter-class differences are also maximized. It is easy to identify the urban built-up area by visual interpretation and computer collaborative computing.

4 Results and Analysis

4.1 Collaborative Computing Results and Precision Evaluation

The urban built-up area and other three types of land covers (i.e., water, green land and agriculture) are obtained by the proposed collaborative calculation method in this paper, and the results is shown in Fig. 4.

In order to test the effect of urban built-up area extracted by the collaborative computing method, in the next, the confusion matrix is used to evaluate the accuracy of classification results of TM remote sensing image in 1988 and 2007, respectively. The results are shown in Tables 2 and 3.

As shown in Tables 2 and 3, the total accuracy of TM image classification in 1988 reached 92.58%, and the Kappa coefficient reached 0.8933. Meanwhile, the total accuracy of TM image classification in 2007 reached 91.41%, and the Kappa coefficient reached 0.8722, respectively. In Fig. 4(a), the water type information is basically

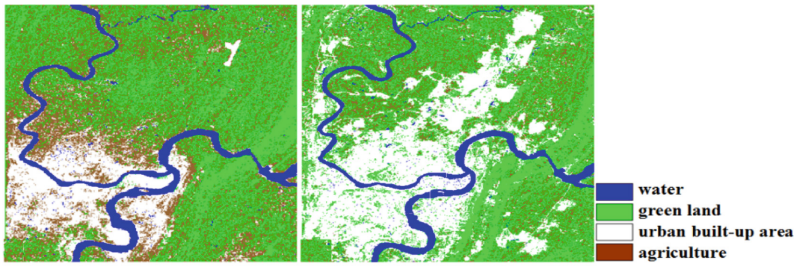

(a) (b)

Fig. 4. Classification results of TM images, (a) 1988, (b) 2007.

Table 2. Error matrix

Time	Type	Water	Urban built-up area	Green land	Agriculture	Total
1988	Water	23	0	0	0	23
	Urban built-up area	0	94	0	9	103
	Green land	0	0	80	4	84
	Agriculture	0	4	2	40	46
	Total	23	98	82	53	256
2007	Water	28	0	2	0	30
	Urban built-up area	0	95	0	4	99
	Green land	0	7	90	5	102
	Agriculture	0	2	2	21	25
	Total	28	104	94	30	256

Table 3. Classification accuracy

Time	Type	Number of reference pixels	Number of classified pixels	Number of corrected classified pixels	Production accuracy	User accuracy
1988	Water	23	23	23	100.00%	100.00%
	Urban built-up area	98	103	94	95.92%	91.26%
	Green land	82	84	80	97.56%	95.24%
	Agriculture	53	46	40	75.47%	86.96%
	Total	256	256	237	–	–
	Total accuracy	92.58%		Kappa coefficient	0.8933	
2007	Water	28	30	28	100.00%	93.33%
	Urban built-up area	104	99	95	91.35%	95.96%
	Green land	94	102	90	95.74%	88.24%
	Agriculture	30	25	21	70.00%	84.00%
	Total	256	256	234	–	–
	Total accuracy	91.41%		Kappa coefficient	0.8722	

extracted accurately, and the accuracy of the producer and the user accuracy reached 100.00%, respectively. There was a certain misclassified between the urban built-up area and the agricultural land, but there are very few mistakes between the green land and agricultural. According to the analysis, it may be caused by the conversion from the initial cultivated land type to the urban built-up area. At the same time, the misclassification between agriculture and green land maybe caused not by some green land but corn and vegetables in agriculture land. In Fig. 4(b), it is similar to the situation in 1988 that the misclassification occurred in the TM remote sensing image (see Fig. 4a). As a whole, with the expansion of urbanization, the landuse type has become more complicated; it led to a slight decrease in the accuracy of TM remote sensing image classification from 92.58% in 1988 to 91.41% in 2007.

(2) Dynamic Changes of Urban Built-Up Area over Time

①*Rate of Urban Built-Up Change*

Landuse information dynamic changes can usually be expressed by the rate of landuse type over time. It can accurately describe the rate of landuse type change, especially in the urban built-up area, and predict the future changes of the landuse information. In fact, there is single landuse dynamic rate and comprehensive landuse dynamic rate.

Single landuse dynamic rate refers to the quantitative change in landuse types over a period of time in an area. And the calculation formula is as shown below:

$$K = (U_b - U_a)/(U_a \times T) \times 100\% \tag{7}$$

where U_a is the number of the initial landuse types, U_b is the number of the end landuse types, T is the time period (i.e., year, month and day). In reality it is also the annual gradient.

Table 4 clearly illustrates the changes in urban built-up areas and other three landuse types obtained during the period 1988–2007 by formula (7).

Table 4. Changes of landuse types during the 1988–2007

	Time	Changes	Water	Urban built-up area	Green land	Agriculture
Divided period	1988–1994	Area (km^2)	−0.13	24.74	−5.21	−19.4
		Proportion (%)	−0.04	2.53	−0.23	−1.00
	1994–2000	Area (km^2)	−2.16	65.34	−22.45	−40.73
		Proportion (%)	−0.61	5.81	−1.00	−2.24
	2000–2003	Area (km^2)	−2.15	34.86	−13.28	−19.43
		Proportion (%)	−1.25	4.60	−1.25	−2.46
	2003–2007	Area (km^2)	−0.22	37.42	−18.87	−18.33
		Proportion (%)	−0.10	3.25	−1.39	−1.88
Whole period	1988–2007	Area (km^2)	−4.66	162.36	−59.81	−97.89
		Proportion (%)	−0.41	5.25	−0.83	−1.59

As shown in Table 4, from the overall change point of view, there is only the urban built-up area increased as well as the other three types of landuse decrease, the area of urban built-up area increased to 162.36 km^2 and the annual change rate reached 5.25%, which is also the largest change rate of the four types of landuse. Thereinto, the water area only slightly decreased, only reduced 4.66 km^2, and the annual change rate reached 0.41%. It can be concluded that in the expansion of urbanization some dispersed and small-sized pools and pits transformed into the urban built-up area. It is also shown in Fig. 5. Second only to the type of urban built-up area, the area of agriculture and green land has decreased by 97.89 km^2 and 59.81 km^2, respectively, and the annual change rates reached 1.59% and 0.83%, respectively. From another point of view, the decrease area of green land and agriculture is basically close to the increased area of urban built-up area. To some extent, it can be considered that the green land and agriculture are the most important sources of urban built-up area transformation in the urbanization.

Table 5. TPM of urban built-up area and other type's landuse

Type		Water	Urban built-up area	Green land	Agriculture	Total
Water	Area (km^2)	48.27	2.94	1.94	1.80	54.95
	Transition probability (%)	87.84	5.35	3.53	3.28	100
Urban built-up area	Area (km^2)	8.27	128.24	77.72	110.83	325.06
	Transition probability (%)	2.54	39.45	23.91	34.10	100
Green land	Area (km^2)	1.49	12.23	181.31	125.55	320.58
	Transition probability (%)	0.46	3.82	56.56	39.16	100
Agriculture	Area (km^2)	1.58	19.29	119.42	84.87	225.16
	Transition probability (%)	0.70	8.57	53.04	37.69	100
Total		59.61	162.70	380.39	323.05	925.75

②*Conversions of Urban Built-up Area and Other Types of Landuse*

In order to calculate and analyze the mutual transformation between urban built-up area and other type's landuse during the period 1988–2007, the transition probability matrix (TPM) method was introduced, and the statistical results are shown in Table 5 and Fig. 5.

As shown in Table 5 and Fig. 5, for the urban built-up area, it has small transfer probabilities to agricultural land, green space and water due to the policy influence of greening construction and overall planning. The conversion between water and urban built-up area, green land and agriculture is small, and the transfer probabilities reached 2.54%, 0.46% and 0.70%, respectively. Meanwhile, the transfer area and probabilities from green land and agriculture to urban built-up area are relatively large, and reached

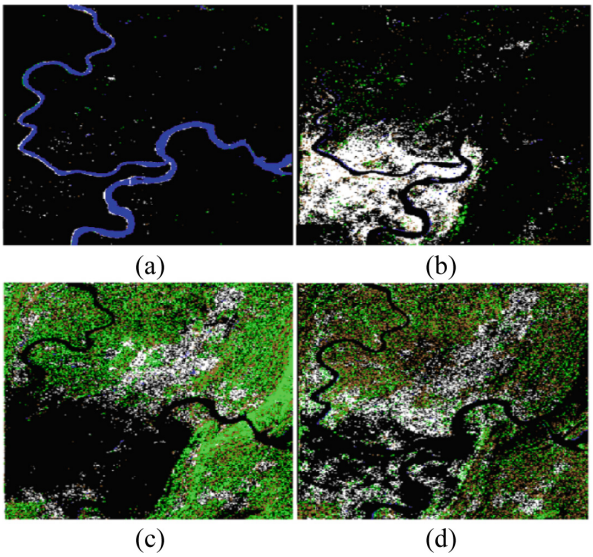

Fig. 5. Transition probability results, (a) water, (b) urban built-up area, (c) green land, (d) agriculture.

77.72 km^2 and 110.83 km^2, respectively, accounting for 23.91% and 34.10% of the total transfer. It also can be verified in Fig. 5(c) and (d). For example, the transfer proportion from green land to agriculture is also large and reached a total of 119.42 km^2, accounting for 53.04% of the total agriculture transfers. In addition, the transferred area from agriculture to the green land reached space by 125.55 km^2, accounting for 39.16% of the total green land transfers. Compared with the field reference data, these transferred area are mainly affected the actual geographical conditions, i.e., topography, slope and environment factors.

(3) Spatial Change in Urban Built-Up Area

①*Gravity Center Changes of Urban Built-Up Area*

The gravity center change model is a commonly used model to describe the spatial distribution of geospatial targets. The center of gravity usually refers to the radial position of the target object, which can keep the target features evenly distributed. In this study, the gravity center change model of urban built-up area distribution is used to invert the whole landuse change in spatial distribution. The spatial center of gravity model can be obtained by weighted averaging of geographic coordinate values, map latitude and longitude. The specific formula is as shown below:

$$\begin{cases} X_t = \sum (C_{ti} \times X_i) / \sum C_{ti} \\ Y_t = \sum (C_{ti} \times Y_i) / \sum C_{ti} \end{cases} \tag{8}$$

where X_t and Y_t are the geographical coordinates of urban built-up area in t-th year, X_i and Y_i are the geometric center coordinate in i-th area, C_{ti} is the area of urban built-up area in i-th area.

Figure 6 demonstrates the gravity center shifting of urban built-up area distribution in study area from 1988 to 2007. It can be clearly seen from Fig. 6 that the gravity center of the urban built-up area has been shifted to the north-east direction. During the period 1988–1994, the offset speed was less than the speed of the matching speed. Since 1994, the offset speed has begun to increase, and reached its maximum by 2000 and then gradually decreasing. By 2003, the offset speed was basically consistent with the matching speed and then again less than the matching speed. According to the analysis, the scale of urban built-up areas expanded at a small rate before 1997 and the distribution center of the built-up areas also changed little. However, the size of the urban built-up area in the study area has expanded dramatically with the strategy of establishing a municipality directly under the central government and the development of the western region, and reached its peak in 2003. Subsequently, the government began to systematically control the expansion speed and scale of the urban built-up area, so the shifting gravity center of the urban built-up area gradually decreased.

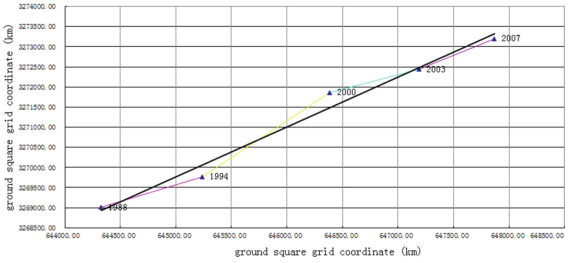

Fig. 6. The shifting gravity center of urban built-up area during the period 1988–2007.

As shown in Fig. 6, the gravity center of the urban built-up area in the study area was shifted by 5.48 km from the north to the east during the period 1988–2007, and the offset angle was 49.7° east. The average offset of the gravity center of the urban built-up area was 0.13 km during the period 1988–1997 as well as the average offset was as high as 0.42 km during the period 1997–2007. It means the urban built-up area has expanded rapidly since the establishment of the Chongqing municipality in 1997.

②*Fractal Feature of Urban Built-Up Area*

Assuming that the urban built-up area is a closed structural unit, the fractal dimension can be expressed by the following formula:

$$D_t = \frac{2\ln(P_t/4)}{\ln(S_t)} \tag{9}$$

where D_t is the fractal dimension, t is the certain time (e.g., year) of statistical urban built-up area, P is perimeter of the unit, S is the area of the unit.

Based on TM images in 1988 and 2007 and assistant data in 1994, 2000 and 2003, respectively, the area and perimeter of urban built-up area of different periods are calculated, and then the corresponding fractal dimension are calculated and counted. In order to systemically research the fractal dimension change of urban built-up area during the periods, the earlier and corrected landuse map in 1983 as well as the latest Chongqing statistics in 2010 published by the bureau were introduced and used in the study. And the fractal dimension of urban built-up area during the period 1988–2007 is shown in Table 6 and Fig. 7.

Table 6. Fractal dimension of urban built-up area

	1983	1988	1994	2000	2003	2007	2010
Fractal dimension	1.5347	1.5411	1.5483	1.5876	1.6324	1.7145	1.7032

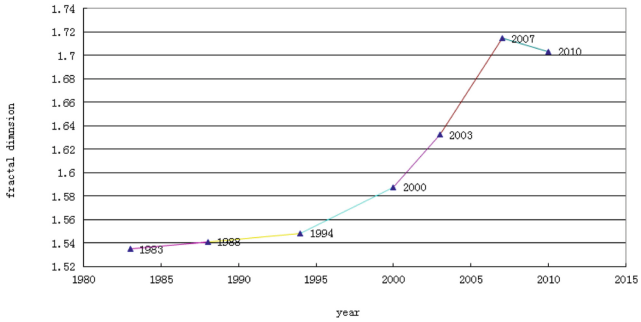

Fig. 7. Fractal feature of urban built-up areas in the study area.

It can be clearly seen from Table 6 and Fig. 7 that the fractal dimensions of the urban built-up area of the study area is greater than 1.5, it indicates that the shape of the urban built-up area is more complicated. In addition, with the large-scale expansion of the urban built-up area and the gradual increase of the fractal dimension, the complexity of the graphic shape of the urban built-up area unit will further increase.

The fractal dimension of the graphic shape of the urban built-up area unit has been floating around 1.54 before 1994. However, it increased rapidly to 1.5876 in 2000, and increased to 1.6324 in 2003 and 1.7145 in 2007. The range of increase was enlarging year by year. When the fractal dimension increases, it indicates that the urban built-up area is dominated by epitaxial expansion. In contrast, when the fractal dimension falls, it indicates that the urban built-up area is dominated by internal filling. Thereinto, the urban built-up area has been in the stage of epitaxial expansion with a slower pace during the period 1983–2007. After the establishment of the Chongqing municipality and the western development strategy, especially in the period 1994–2000, the scale of the urban built-up area in the study area expanded rapidly, and the expansion mode of the urban built-up area was accompanied by simultaneously the extension and internal filling, only the extension of the extension was more obvious. After a period of rapid

expansion, the expansion focus of urban built-up areas began to shift to internal filling by 2007. Meanwhile, the fractal dimension of the graphic shape of the urban built-up area began to show a trend of slight downward.

(4) Affecting Factors of Urban Built-Up Area Change

The socio-economic development and population increase are the most important driving factors for the expansion of urban built-up areas. Among them, economic development is the fundamental driving factor for the expansion of urban built-up areas, and the increase of population is the external driving factor for the expansion of built-up areas.

①*Economic Factors*

The relationship between urban built-up area and gross domestic product (GDP) in the study area during the period 1988–2010 is shown in Fig. 8.

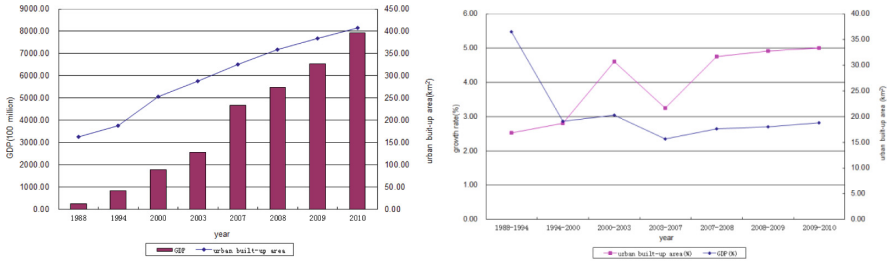

(a) (b)

Fig. 8. Relationship between urban built-up area and GDP, (a) urban built-up area and GDP, (b) growth rate of urban built-up area and GDP.

As shown in Fig. 8, the urban built-up area and GDP have grown at a high speed from 1988. Although there are differences between different years, the overall growth trend tends to be the same. On the one hand, the growth rate of urban built-up area during the period 1988–1994 was relatively small. After 1994, especially the establishment of municipality in 1997, the economy developed rapidly and the urban built-up area also maintained a high growth rate. When the urban built-up area has expanded to a certain scale, its growth rate has slightly decreased, and then it has begun to stabilize. On the other hand, the GDP growth rate during the period 1988–1994 was much higher than that of earlier years, and the GDP growth is basically in line with the growth of urban built-up areas since 1994. Subsequently, GDP had a small peak in growth in 1997 and 2000; meanwhile, the GDP began to grow at a relatively steady rate.

②*Population Factors*

Figure 9 shows the relationship between the population and the built-up area during the period 1988–2007.

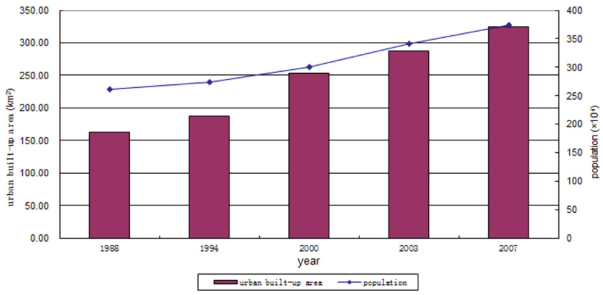

Fig. 9. Relationship between population and urban built-up area.

As shown in Fig. 9, there is a clear positive correlation between the population and the urban built-up area during the period 1988–2007. Similar to the expansion of the urban built-up area, the population growth rate of the study area is relatively low before the establishment of municipality in 1997. By 1997, especially in 2000, there has been a corresponding inflection point in population growth, and then it has entered a high-speed increase phase. At present, with the implementation of the reform of the urban and rural areas policy, as well as the increasing attractiveness of the city itself, it is estimated that the rapid growth in population can continue for some time.

5 Discussions

Aiming at the current insufficiency of identification accuracy of urban built-up area from remote sensing data and selecting thresholds, this paper proposed a new method for collaborative computing of urban built-up area from remote sensing image. It successfully introduced the idea of collaborative computing into the remote sensing data mining. Compared with the traditional identified methods, the proposed collaborative computing method has a great improvement in space-time accuracy and computational efficiency. And the value is mainly reflected in the following aspects:

(1) Combining with the idea of collaborative computing, the map-spectrum synergy, multi-temporal and multi-source remote sensing data synergy are introduced in the identification an extraction of urban built-up area from remote sensing image. The application value of the collaborative computing proposed in this paper is proved by the specific built-up area identification and extraction in Chongqing case.

(2) Aiming at the segmentation threshold in the extraction of urban built-up area, the automatic identification of urban built-up area by map-spectrum collaborative computing, and finally realizes the statistics of urban built-up area by mathematical morphology method are completed. To a certain extent, it avoids the selection of segmentation threshold in the traditional method. The experimental results show that the identification of the urban built-up area by proposed method are not only high overall accuracy and have small errors, but also the results are basically consistent with the visual interpretation range.

(3) This study realizes the rapid, efficient and accurate identification of urban built-up area at small scales. At the same time, by analyzing the spatial and temporal dynamic changes, development trends and influencing factors of urban built-up areas in Chongqing case, it has certain reference value for the identification and extraction of other district from remote sensing data.

6 Conclusions

Based on the traditional identification and extraction methods of urban built-up area, this paper proposed a collaborative computing method for urban built-up area identification from remote sensing image. The NDVI and NDBI are constructed by the collaborative computing of map-spectrum, multi-temporal remote sensing data, multi-knowledge and auxiliary data, and further the urban built-up area in 1988 and 2007 was identified an extracted from TM remote sensing images by mathematical morphology. The experimental results show that:

(1) The total accuracy of urban built-up areas identification of Chongqing municipality in 1988 and 2007 reached 92.58% and 91.41%, respectively, and the Kappa coefficients reached 0.8933 and 0.8722, respectively.
(2) The increased area of urban built-up area reached 162.36 km^2, and the annual change rate is 5.25%. The enlarged area is mainly transformed from cultivated land, woodland, grassland and waters.
(3) The gravity center of the urban built-up area in Chongqing municipality was shifted by 5.48 km from the north to the east during the period of 1988–2007, and the offset angle reached 49.7°.
(4) The fractal dimension of the urban built-up area during the period of 1988–2007 is greater than 1.5; it indicates that the graphic shape of the urban built-up area is more complicated. With the large-scale expansion of the urban built-up area, the fractal dimension of the urban built-up area will be further increased.
(5) It is further verified that socioeconomic development and population increase are the most important driving factors for the expansion of urban built-up area. And there is a clear positive correlation between urban built-up area and the growth of economy and population.

On the basis of collaborative computing proposed in this paper, the collaborative computing mode combined multi-source, multi-temporal, multi-knowledge and computing resources with the characteristics of remote sensing images will be our focus in the future.

Acknowledgements. This research was supported by the National Natural Science Foundation of China under Grant No. U1811461, Graduate Innovation and Entrepreneurship Program in Shanghai University in China under Grant No. 2019GY04, Science and Technology Development Foundation of Shanghai in China under Grant No. 16dz1206000 and 17dz2306400.

References

1. Li, Z., Yang, X.M., Meng, F., Chen, X., Yang, F.S.: The method of multi-source remote sensing synergy extraction in urban build-up area. J. Geo-Inf. Sci. **19**(11), 1522–1529 (2017)
2. Cheng, Y., Zhao, L., Wan, W., Li, L.L., Yu, T., Gu, X.F.: Extracting urban areas in china using DMSP/OLS nighttime light data integrated with biophysical composition information. J. Geogr. Sci. **26**(3), 325–338 (2016)
3. Li, G.D., Fang, C.L., Wang, S.J., Zhang, Q.: Progress in remote sensing recognition and spatio-temporal changes study of urban and rural land use. J. Nat. Resour. **31**(4), 703–718 (2016)
4. Xu, Z.N., Gao, X.L.: A novel method for identifying the boundary of urban built-upareas with POI data. Acta Geographica Sinica **71**(6), 928–939 (2016)
5. Li, X.M., Zheng, X.Q., Yuan, T.: Knowledge mapping of research results on DMSP/OLS nighttime light data. J. Geo-Inf. Sci. **20**(3), 351–359 (2018)
6. Ma, T., Zhou, C.H., Pei, T., Fan, J.: Quantitative estimation of urbanization dynamics using time series of DMSP/OLS nighttime light data: a comparative case study from China's cities. Remote Sens. Environ. **124**(1), 99–107 (2012)
7. Small, C., Elvidge, C.D., Balk, D., Montgomery, M.: Spatial scaling of stable night lights. Remote Sens. Environ. **115**(2), 269–280 (2011)
8. Gong, P., Li, X., Xu, B.: Interpretation on theory and application method development for information on extraction from high resolution remotely sensed data. J. Remote Sens. **10**(1), 1–5 (2006)
9. Zhang, T., Yang, X.M., Tong, L.Q., He, P.: Selection of best-fitting scale parameters in image segmentation based on multiscale segmentation image database. Remote Sens. Land Resour. **28**(4), 59–63 (2016)
10. Li, D.R., Zhang, L.P., Xia, G.S.: Automatic analysis and mining of remote sensing big data. Acta Geodaetica Cartographica Sinica **43**(12), 1211–1216 (2014)
11. Li, C.F., Liu, L., Sun, X.K., Zhao, J.J., Yin, J.Y.: Image segmentation based on fuzzy clustering with cellular autimata and features weighting. EURASIP J. Image Video Process. **1**, 36 (2019)
12. Chen, S.P., Yue, T.X., Li, H.G.: Studies on geo-informatic Tupu and its application. Geogr. Res. **19**(4), 337–343 (2000)
13. Luo, J.C., Wu, T.J., Xia, L.G.: The theory and calculation of spatial-spectral cognition of remote sensing. J. Geo-Inf. Sci. **18**(5), 578–589 (2016)
14. Shen, Z.F., Li, J.L., Yu, X.J.: Water information extraction of Baiyangdian wetland based on the collaborative computing method. J. Geo-Inf. Sci. **18**(5), 690–698 (2016)
15. Ming, D.X., Luo, J.C., Shen, Z.F., Wang, M.M., Sehng, H.: Research on information extraction and target recognition from high resolution remote sensing image. Sci. Surveying Mapp. **30**(3), 18–20 (2005)
16. Li, S.J., Tao, J., Wan, D.S., Feng, J.: Content-based remote sensing image retrieval using co-training of multiple classifiers. J. Remote Sens. **14**(3), 493–506 (2010)
17. Ma, Y., et al.: Remote sensing big data computing: challenges and opportunities. Future Gener. Comput. Syst. **51**(1), 47–60 (2015)
18. O'Callaghan, J.F., Mark, D.M.: The extraction of drainage networks from digital elevation data. Comput. Vis. Graph. Image Process. **28**(2), 323–344 (1984)
19. Lu, D., Tian, H., Zhou, G., Ge, H.L.: Regional mapping of human settlements in southeastern China with multisensor remotely sensed data. Remote Sens. Environ. **112**(9), 3668–3679 (2008)

20. Iounousse, J., Er-Raki, S., Chehouani, H.: Using an unsupervised approach of probabilistic neural network (PNN) for land use classification from multitemporal satellite images. Appl. Soft Comput. **30**(1), 1–13 (2015)
21. Knight, A., Tindall, D., Wilson, B.: A multitemporal multiple density slice method for wetland mapping across the state of Queensland, Australia. Int. J. Remote Sens. **30**(13), 3365–3392 (2009)
22. Zhou, Y., Qiu, F.: Fusion of high spatial resolution WorldView-2 imagery and LiDAR pseudo waveform for object-based image analysis. ISPRS J. Photogramm. Remote Sens. **101** (1), 221–232 (2015)
23. Zhao, R.B., Zhao, S.H., Hu, X.L.: A CPU-GPU collaboration based computing parallel algorithm for MTF degradation of remote sensing simulation images. Comput. Eng. Sci. **37**(7), 1258–1264 (2015)
24. Zhang, Q., Schaaf, C., Seto, K.C.: The vegetation adjusted NTL urban index: a new approach to reduce saturation and increase variation in nighttime luminosity. Remote Sens. Environ. **129**(1), 32–41 (2013)